



**Status report on the WP2 of the
Swiss-Danish instrumentation work packages
for the European Spallation Source, ESS**

focusing reflectometer (Selene)

J. Stahn, August 12, 2012



Paul Scherrer Institut



| | | |
|-------------|-----|--|
| Switzerland | PSI | Jochen Stahn Panagiotis Korelis Uwe Filges Tobias Panzner |
| Denmark | CU | Marité Cardenas Ursula Hansen |
| | USD | Beate Klösgen |

project team

Jochen Stahn senior scientist
Laboratory for Neutron Scattering
Paul Scherrer Institut
Switzerland
jochen.stahn@psi.ch
+41 56 310 2518

Panagiotis Korelis pst-doc
Laboratory for Neutron Scattering
Paul Scherrer Institut
Switzerland
panagiotis.korelis@psi.ch
+41 56 310 5813

Uwe Filges senior scientist
Laboratory for Developments and Methods
Paul Scherrer Institut
Switzerland
uwe.filges@psi.ch
+41 56 310 4606

Tobias Panzner pst-doc
Laboratory for Developments and Methods
Paul Scherrer Institut
Switzerland
tobias.panzner@psi.ch
+41 56 310 4342

Marité Cardenas senior scientist
Nano-Science Center
University of Copenhagen
cardenas@nano.ku.dk
+45 35 320 431

Ursula Bengaard Hansen student assistant
Nano-Science Center
University of Copenhagen
ursulabengaard@gmail.com
+45 50 90 96 67 (mobile)

Beate Klösgen associate Professor
MEMPHYS, Department for Physics, Chemistry and Pharmacy
University of Southern Denmark
Denmark
kloesgen@sdu.dk
+45 6550 2561

Selene



detail of the ceiling painting
Selene and Endymion
at the *Ny Carlsberg Glyptotek*, Copenhagen

Contents

| | | |
|----------|---|-----------|
| 1 | introduction | 5 |
| 2 | the generic focusing reflectometer | 6 |
| 2.1 | moderator | 8 |
| 2.2 | beam extraction | 9 |
| 2.2.1 | elliptic feeder | 9 |
| 2.2.2 | double-bandpass partly within extraction unit | 10 |
| 2.2.3 | pin hole | 11 |
| 2.3 | <i>Selene</i> guide system | 12 |
| 2.3.1 | angular acceptance | 12 |
| 2.3.2 | coma aberration — and correction | 12 |
| 2.3.3 | chromatic aberration due to gravity | 13 |
| 2.3.4 | length of the guide system | 14 |
| 2.3.5 | technical aspects | 14 |
| 2.3.6 | comparison to a straight guide | 14 |
| 2.4 | sample area | 16 |
| 2.5 | detector | 17 |
| 3 | reflectometer for tiny samples | 18 |
| 3.1 | double- <i>Selene</i> guide system | 19 |
| 4 | reflectometer with a horizontal sample surface | 22 |
| 4.1 | ... as an option on a straight guide | 23 |
| 5 | prototype | 25 |
| 5.1 | BOA | 25 |
| 5.2 | design considerations | 25 |
| 5.3 | devices | 25 |
| 5.3.1 | pulse chopper | 25 |
| 5.3.2 | frame overlap chopper | 26 |
| 5.3.3 | precision slit | 26 |
| 5.3.4 | double multilayer monochromator | 26 |
| 5.3.5 | sample holder | 26 |
| 5.3.6 | guide support | 27 |
| 5.3.7 | guide system | 27 |
| 5.4 | set-up | 27 |
| 5.5 | experiments | 28 |
| 6 | publications | 29 |
| 7 | schedule | 31 |

| | | |
|----------|---|-----------|
| A | geometrical considerations for an elliptic reflector | 32 |
| A.1 | length of guide system | 34 |
| A.2 | gravity | 35 |
| B | operation modes | 36 |
| B.1 | almost conventional | 36 |
| B.2 | high-intensity specular reflectivity | 36 |
| B.2.1 | off-specular and incoherent scattering | 37 |
| B.3 | low-divergent beam | 38 |
| B.4 | small spot size | 38 |
| B.5 | wide q -range | 39 |
| B.6 | angle/energy encoding | 40 |
| B.7 | high q_z -resolution | 41 |
| B.8 | pure TOF | 41 |
| C | double multilayer monochromator | 42 |
| D | frame-overlap and polarisation filter | 43 |
| E | chopper options – resolution | 44 |
| E.1 | no chopper | 44 |
| E.2 | quasi double blind chopper | 44 |
| E.3 | repetition rate multiplication | 44 |

1 introduction

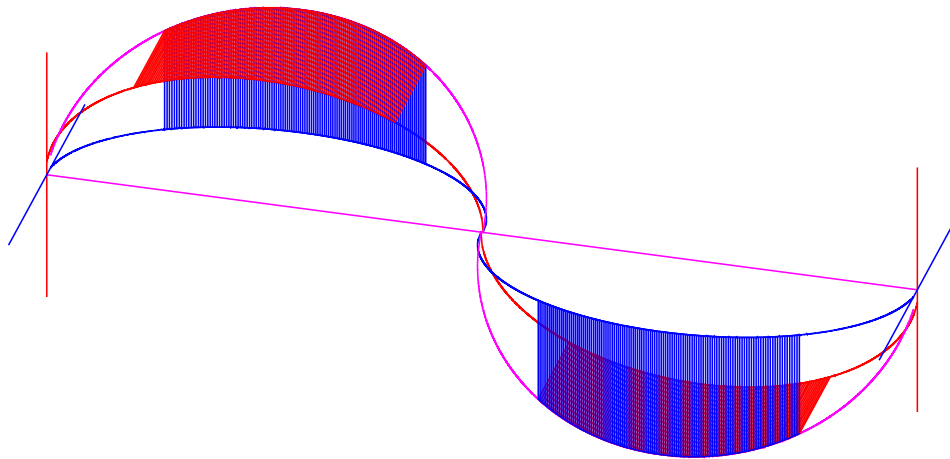
The *Swiss-Danish Instrument Initiative* proposes to build several, but highly optimised instruments of one class, rather than one flexible instrument with moderate performance due to the necessary compromises. As “guiding ideas” we suggest I a small sample size, II a horizontal sample interface, and eventually III high resolution in q_y (i.e. GISANS).

Optimisation requirements of I and II exclude each other to some extent: The vertical scattering plane imposes quite severe constraints for high-angle diffraction, and gravitation effects become important. On the other side typical samples with liquid/liquid or liquid/gas interfaces are larger than $10 \times 10 \text{ mm}^2$, while really *small* samples are the order $100 \times 100 \mu\text{m}^2$.

A generic reflectometer is designed on the basis of using elliptically shaped guides and focusing to the sample in both directions normal to the beam (section 2).

The usage of point-to-point focusing rather than a straight guide leads to a drastically reduced beam intensity in the guide, while almost conserving the phase space density actually needed for the measurements. Also the beam is convergent at the sample which avoids over-illumination of the sample (if required) and of the sample environment.

The idealised set-up consists of two subsequent identical guides (see sketch below and figure 1). Each guide has one reflecting surface shaped like one branch of an ellipse for each direction (like a Montel optics as used at synchrotron beam line).



The (virtual) source is mapped by the first guide to an intermediate image, which is then mapped to the sample position. This way the coma aberration inherent to elliptic reflectors is almost completely corrected for. The maximum divergence $\Delta\theta$ is given by the acceptance of the first ellipse. It can be reduced by an aperture in between the focal planes. The spot-size at the sample position is (almost) identical to the source size, i.e. it can be adjusted by slits at the first focal point without changing $\Delta\theta$.

With reference to the half-elliptical shape of the light-to-shadow border on the moon we call this the *Selene* set-up.

In the following sections the generic lay-out of the instrument is presented, followed by discussions of its components from source to detector. Based on these considerations two possible realisations for the ESS are presented, one optimised for small samples (with horizontal scattering plane, section 3) and one optimised for liquid interfaces (section 4). The design and realisation of a prototype *Selene* guide is presented in section 5.

2 the generic focusing reflectometer

We develop a reflectometer for the ESS using a beam focused both, in the sample plane, and in the scattering plane. The generic instrument has the following lay-out in the scattering plane:

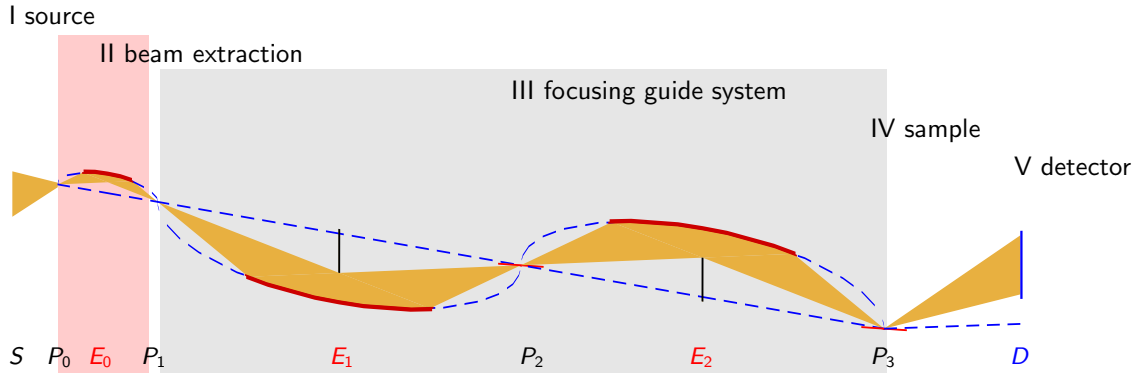


Figure 1: generic lay-out of the focusing reflectometer (*Selene*): Cut in the scattering plane, stretched by 10 normal to incident beam.

I source (section 2.1): The instrument needs a cold moderator as neutron source, where the effective flux maximum (i.e. including losses and rescaling) determines the minimum wavelength used λ_{\min} .

II beam extraction (2.2): Technical and spatial constraints and the high radiation level close to target and moderator prohibit the installation of moving or adjustable equipment within the first 6 m. Thus a beam extraction device is needed to create a virtual source with a sufficiently high and homogeneous $\Delta\theta$ and size outside the *biological shielding*. The design of this part should reduce the fast neutron and γ doses as much as possible.

III focusing guide system (2.3): Between the virtual source and the sample a focusing guide system is realised, based on the *Selene* concept. I.e. the pre-image defined by an aperture of the size of the required footprint (located at P_1) is mapped to the sample area (P_3). This is realised by two subsequent reflectors of elliptic shape (E_1 and E_2) which share a focal point (P_2).

The two subsequent ellipses create a beam converging to the sample with a cross section at P_3 with almost the same measures as the slit at P_1 . The second ellipse almost completely corrects for the coma aberration of the first one. In addition the usage of two ellipses reduces the lateral extension of the guide. It allows for a convenient beam manipulation close to P_2 , where the beam is small (several mm^2 , only). And by de-tuning E_2 relative to E_1 one can create either an almost parallel beam or a tiny beam spot at P_3 .

Additional beam-defining elements like slits, choppers, polarisers, and monochromators, can be located in the spaces between P_1 and E_1 , between E_1 and E_2 and behind E_2 . Typically the length of the guide is about half the focal distance, which leaves a lot of free space.

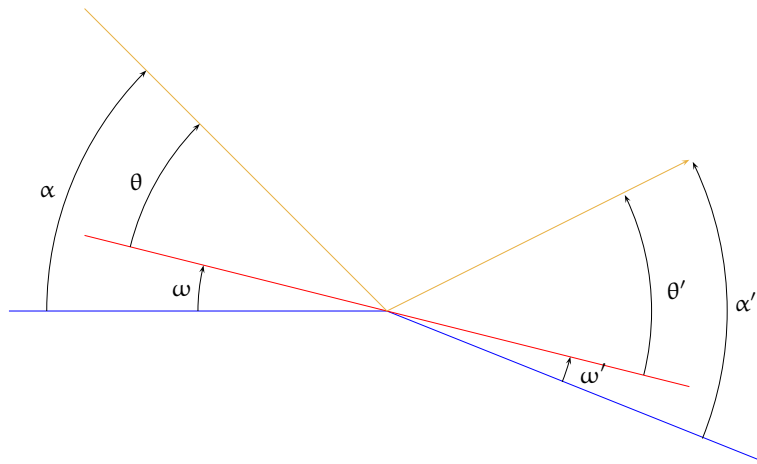
To avoid direct line of sight to the source, a beam-stop is located in the middle of E_1 . A strong shielding is only required till the end of E_1 . But even there the radiation level should be quite small because of the small dimensions of the slit at P_1 .

IV sample (2.4): The sample is located at the second focal point P_3 of the second ellipse E_2 .

V detector (2.5): A position sensitive detector is needed, where its angular resolution dominated the resolution of this instrument concept. For diffraction a second, shorter detector arm allowing for $2\theta \leq 140^\circ$ can be installed.

Table 1: For the description and discussion in the next sections the following nomenclature is chosen:

| | |
|---|----------------------------------|
| focal points of the ellipses | $P_{1,2,3}$ |
| source reference point | S |
| detector reference point | D |
| angle of a reflecting surface at (or close to) $P_{1,2,3}$ relative to the reference line before $P_{1,2,3}$ | $\omega_{1,2,3}$ |
| ... corresponding angle behind $P_{1,2,3}$ | $\omega'_{1,2,3}$ |
| angle $\angle(SP_1P_2)$ | $\eta_{1,2,3}$ |
| angle of incidence (finite angle) of a neutron beam on a reflecting surface | $\theta_{1,2,3}$ |
| ... corresponding finite angle | $\theta'_{1,2,3}$ |
| angle of the neutron beam relative to the reference line before $P_{1,2,3}$ | $\alpha_{1,2,3}$ |
| ... corresponding angle after $P_{1,2,3}$ | $\alpha'_{1,2,3}$ |
| i.e. | $\alpha_i = \omega_i + \theta_i$ |
| the reference line connects S , (P_0), P_1 , P_2 , P_3 , and D | |



2.1 moderator

task: deliver high neutron flux and a sufficient divergence in the requested λ range

The reflectometers using a *Selene* type guide system will not profit from wavelengths shorter than some 2.5 Å because the transported divergence and intensity is decreased too much by the guide. This means that a cold moderator is needed. As derived below the optimal minimum wavelength is of the order of 4 Å to 5 Å, which means that the instrument might profit from a Be-reflector moderator.

The experience with existing TOF reflectometers is, that the lower limit of the wavelength spectrum λ_{\min} corresponds to the effective flux maximum at the sample position. The reason is that small λ result in higher q_z and thus in general in lower reflectivity, and at the same time in a lower incident intensity. Thus the accuracy of the data rapidly decreases and it is much more appropriate to measure a further curve at a higher angle of incidence to access the corresponding q_z range.

The effective flux at the sample can be estimated by reducing the initial flux $I_0(\lambda)$ by the losses due to reflections on the guide walls, and by taking into account that in the end one aims for $\Delta q/q = \text{constant}$ or something quite close.

The guide concept presented further down involves 4 reflections for all neutrons on surfaces with a non-perfect reflectivity R (plus further reflections in the extraction unit). Since the angle of incidence on the guide surface hardly varies for the presented concept, one can assume an attenuation of $R^n(\lambda, m)$ for a guide coating defined by its critical edge $q^c = mq_{\text{Ni}}^c$. This pushes the flux maximum to higher λ .

For the example given in figure 2 we chose a linear decrease of R with λ :

$$R(\lambda, m) = \begin{cases} 1 & \text{for } \lambda > m\lambda_{\min} \\ 0 & \text{for } \lambda < \lambda_{\min} \\ \frac{7 \cdot 0.5}{6} - \frac{0.5}{6} \frac{m\lambda_{\min}}{\lambda} & \text{else} \end{cases} \quad (2.1)$$

(i.e. 50% reflectivity at $m = 7$ and 100% at $m = 1$).

A more prominent effect has the required $\Delta q/q = \text{constant}$: effectively the time-bins, and thus the λ -bins necessary for $R(q_z)$ curves follow $\Delta\lambda/\lambda = \text{const}$ which shifts the spectral weight to the bins with large λ .

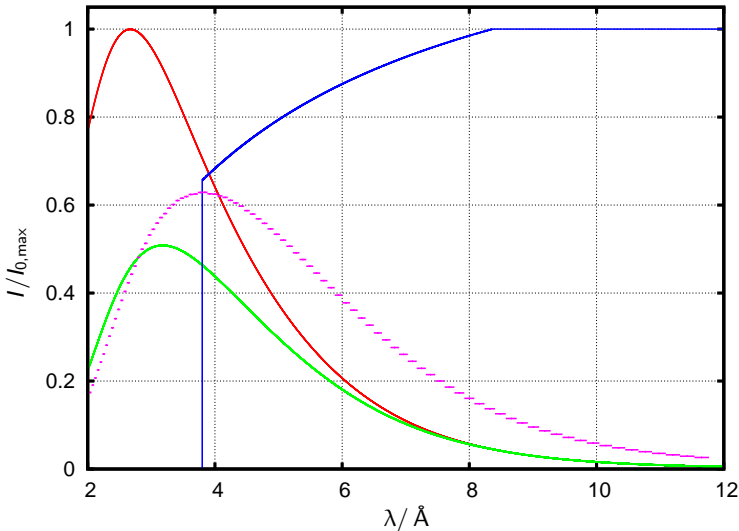


Figure 2: Spectra $I(\lambda)$ as given by the source (red), after attenuation according to eqn. (2.1) with 4 reflections (green), and after rebinning it to $\Delta\lambda/\lambda = 2\%$ (magenta). The latter line is scaled by an arbitrary value. The blue line is the transmission of the guide. For the graphs shown the parameters are $m = 2.2$, $\lambda_{\min} = 3.8 \text{ \AA}$. The source spectrum $I_0(\lambda)$ is the one used by the McStas component `ESS_moderator_long`.

The choice of the proper m and thus λ_{\min} depends on the acceptance of the guide system $\Delta\theta$, and on the λ range. Optimisation is thus an iterative process, where the figure of merit could be the minimisation of the measurement time on a small sample to reach a defined accuracy.

In case the width of the q_z -range covered within one pulse is essential, one might accept also a smaller λ_{\min} for the cost of a dramatically increased measurement time.

2.2 beam extraction

task: transport the requested phase space volume outside the biological shielding, while reducing the radiation as much as possible

Disregarding technical aspects and neighbored instruments, the ideal lay out of the beam guide would start with an adjustable aperture close to the source (in a way to collect the needed divergence). Directly afterwards a small chopper would be installed, allowing to mimic a double blind chopper. The actual guide (E_1) then starts several meters down-stream.

But the constraints at the ESS prevent this:

- A containment wall at $x = 2$ m does not allow any optics or shielding closer to the moderator.
- The shutter within the biological shielding makes it difficult (or impossible) to manipulate a slit or even to operate a chopper in front of it.
- Safety considerations may hinder the operation of a relatively fast running chopper within the biological shielding.
- For safety and maintenance reasons, no access to elements within the biological shielding will be allowed.
- The high radiation (neutrons and x-rays) most likely destroys *complex* devices close to the source within a short time.
- The high γ and fast neutron radiation demands for additional shielding outside the biological shielding.

In the *worst case* a minimum distance $\overline{SP_1} > 6$ m has to be taken into account. A *Selene*-type guide system is still possible, but the option of an early chopper is not given, and more important, a wide white beam is guided outside the biological shielding, where it then is reduced dramatically by the first slit. As a consequence much more shielding will be needed outside.

On the other side beam manipulation close to P_1 gets much more convenient. It might even be possible to install a ML monochromator or some reflecting filter there.

2.2.1 elliptic feeder

Figure 3 shows a possible lay-out of the beam extraction including source and first optical elements at P_1 . An additional short elliptic guide bridges the distance from the inner wall of the biological shielding to P_1 . Coma aberration of this short guide would spoil the phase space if its entrance slit would also be small. To get a homogeneous $I(\lambda, \alpha, z)$ at P_1 an aperture at P_0 of some 10 mm is required. A free space of about 1 m length around P_1 is needed for a slit system, the fast running choppers for repetition rate multiplication, and eventually some filtering optics. The instrument shielding extends along the guide E_1 . Direct line of sight to the source is already blocked by E_0 , and again from P_2 to P_1 by E_1 .

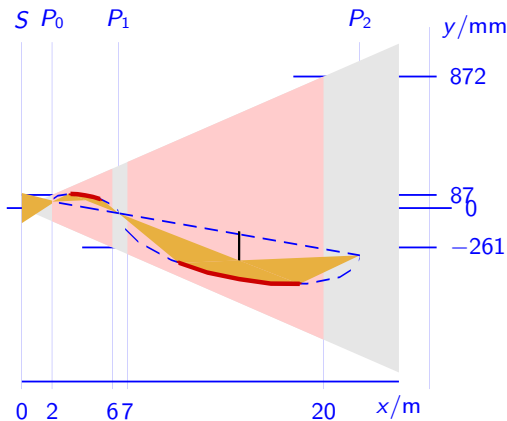


Figure 3: Schematic lay-out of beam extraction and first guide of the reflectometer with a horizontal scattering plane. The light red shaded area are the regions for the biological and the instrument shielding. In between there is a gap of 1 m for an adjustable aperture, choppers, and eventually some filter. The gray wedge corresponds to a 5° segment.

2.2.2 double-bandpass partly within extraction unit

For the operation mode with a band-pass multilayer reflector for λ/θ encoding (section B.6) one could install the first bandpass within the biological shielding. The sketch in figure 4 shows a conceptual study with realistic, but not optimised parameters.

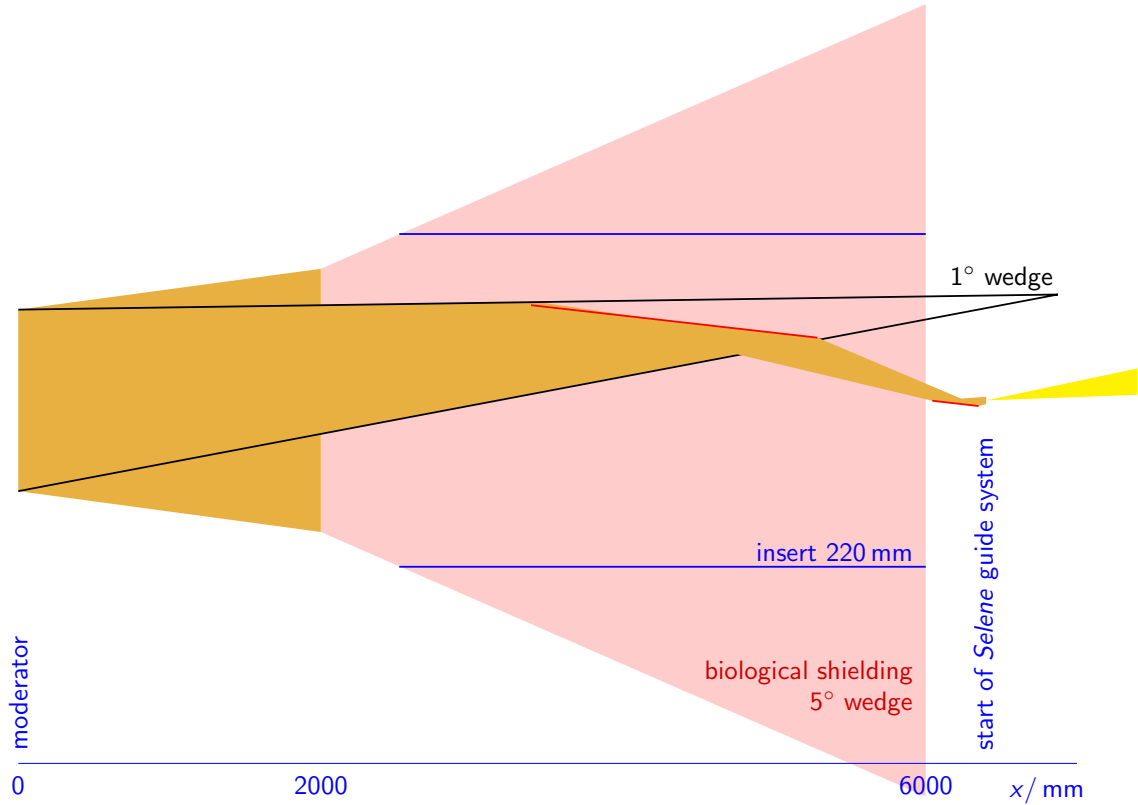


Figure 4: Sketch of the beam extraction unit with the first part of a double ml monochromator built in. The guiding parameters for this sketch are $\Delta\theta = 1^\circ$ (i.e. $\overline{SP}_1 \leq 6874$ mm), $\lambda = [4, 9] \text{ \AA}$, and $\Delta\lambda/\lambda = 10\%$. The first red line represents a band-pass (multilayer, $m = 2$, $\Delta q/q = 10\%$), and the second one outside the shielding is a variable band-pass ($m = 2$, possibly polarising). Here direct line of sight to the moderator is just avoided. Optimisation in coating and distances can improve the situation.

The location of the second bandpass filter is flexible with respect to the first bandpass filter, and with respect to the first focal point of the guide system P_1 . This means that it can be used to correct for misalignment of the order of 10 mm without reducing the performance. A correction in angle is also possible, but on the cost of the available divergence.

To still be able to use the high-intensity specular reflectivity mode (subsection B.2) one might exchange the bandpass filters with supermirror reflectors. This implies a translation of an up to 2 m long element within the biological shielding. An other approach would be to combine the concepts presented here and in the previous subsection, sharing the focal point P_1 and the beam direction. This can be realised with an insert extracting two beams, where one is blocked with the shutter.

In the vertical (y -, sample-) plane, a higher divergence is desirable and can be realised with a rather short parallel guide section. The example shown in figure 5 assumes $\Delta\theta_y = 2^\circ$ for a 20 mm wide spot at P_1 . As a result the guide with 60 mm width starts 1145 mm upstream and it is 2384 mm long. From its entrance the shielding opens towards the source to reach 80 mm at the beginning of the biological shielding. The guide coating has to be $m = 2.5$ for $\lambda_{\min} = 2.5 \text{ \AA}$. Higher divergences are difficult to realise, since the guide will reach closer to the source.

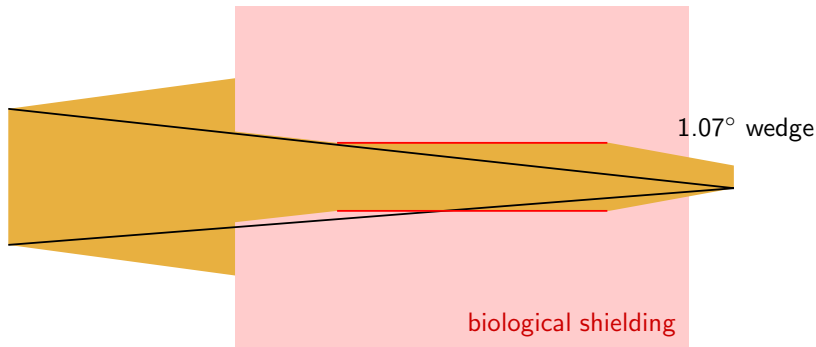


Figure 5: Cut through the beam extraction unit in the plane of the sample surface (xy plane).

2.2.3 pin hole

In case the 6 m radius for the biological shielding is (much) too weak to reduce the γ and fast neutron background, it might be favourable to build a guide with 2 *Selene* sections, i.e. 4 subsequent elliptic guides. In this case the precision beam definition can be realised in between the 2 *Selene* sections - and a fix first aperture can be installed in the biological shielding. There is than direct line of sight to the moderator from outside the biological shielding, but the (also well shielded) first 2 ellipses bent the beam 2 times so that direct and first indirect line of sight is blocked at its end. Figure 6 illustrates the extraction part. The full instrument using 2 *Selene* sections is discussed in section 3.1.

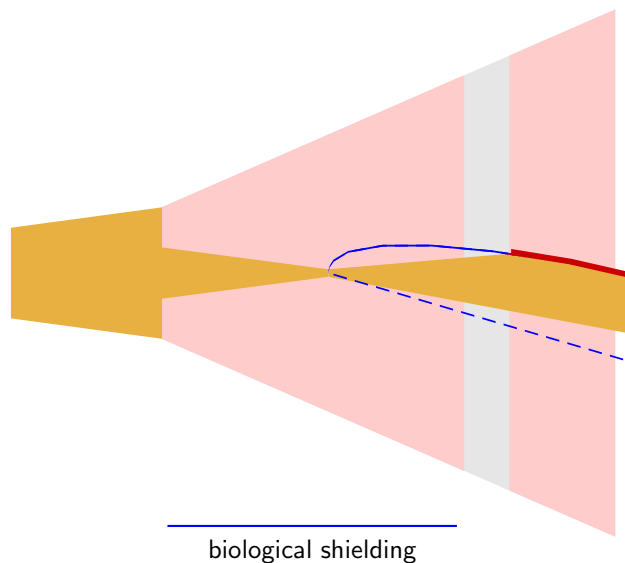


Figure 6: Sketch of a possible extraction section with a pin hole. A small ($10 \times 10 \text{ mm}^2$) aperture some 4.2 m from the source acts as the initial focal slit for the first *Selene* guide section. This position allows for a divergence of $\Delta\theta_{xy} = \Delta\theta_{xz} = 1.5^\circ$. The openings of the flight path section are 68 mm / 58 mm at the entrance / exit of the biological shielding. Between the biological shielding and the entrance of the *Selene* guide there is a gap of 600 mm which e.g. can be used to position a chopper.

3 reflectometer for tiny samples

The flux available at the ESS is mainly used to go for smaller samples. In this case we aim for a footprint size from $10 \times 10 \text{ mm}^2$ down to $0.3 \times 0.3 \text{ mm}^2$.

This sets high limits for the quality of the guides and the possibility to align them. Since the focal spot size is given solely by the initial slit size, the de-tuning of the two guides (sections B.4 and B.3) and the surface fidelity of the guide, there is no possibility to reduce the beam spot with slits after the end of the guide system.

Since for very small samples it will still be difficult to reach high q_z or large dynamic ranges, the option of a full-convergent beam geometry (B.2) is ideally suited for this application.

- *horizontal scattering plane*
 - gravity is a minor issue (affects y -direction, only);
 - allows for high-angle diffraction (to characterise the crystalline quality of thin films);
- cold moderator ($\lambda \geq 4 \text{ \AA}$);
- variable initial slit $[0.1 \dots 2] \times [1 \dots 10] \text{ mm}^2$
 - to define an adaptable small beam spot for scanning;
 - to avoid drastic over-illumination of the sample;
- resolution settings
 - using a ml-monochromator and λ - θ -encoding one gets $\Delta\lambda/\lambda = \text{const}$, adjustable between 2% and 20%.
The same resolutions can be reached by 2 pairs of choppers in between P_1 and E_1 .
 - high ($\Delta q_z/q_z \approx 1\%$) or medium ($\Delta q_z/q_z = \text{const.} \approx 4\%$) can be realised with fast-running choppers at P_1 and P_2 ;
- q_z -range
if a wide q_z range for one instrument setting is required, one can combine λ_{\min} and θ_{\max} , and λ_{\max} and θ_{\min} by either using the full convergent mode (B.2), the variable θ mode (B.5), or the λ - θ -encoding (B.6).
- wavelength band assuming for the moment $4 \text{ \AA} < \lambda < 9 \text{ \AA}$
- dimensions

| | | |
|-------------------|-----------------------------|---|
| source – P_1 | 6.5 m | space between guides space before sample high-angle diffraction vs. high resolution |
| P_1 – P_2 | 16.0 m | |
| P_2 – P_3 | 16.0 m | |
| E_1 – E_2 | 5.3 m | |
| E_2 – P_3 | 2.6 m | |
| P_3 – detector | $[1.5 \dots 7.5] \text{ m}$ | |
| source – detector | $[40 \dots 46] \text{ m}$ | |

$\pm 2.4^\circ$ tilt of E_2 around P_2 ($\pm 0.7 \text{ m}$ translation of P_3).
- polarisation and polarisation analysis (by a polarising SM at P_1 , or P_2 , or by a polarising guide, and a ^3He or SM analyser);
- options
 - MIEZE (coils behind E_1 , and E_2)
 - SERGIS (between E_2 and sample)
 - cryo-magnet
 - high-angle diffraction (2nd detector)

Figure 9 shows a possible layout and measures for this instrument.

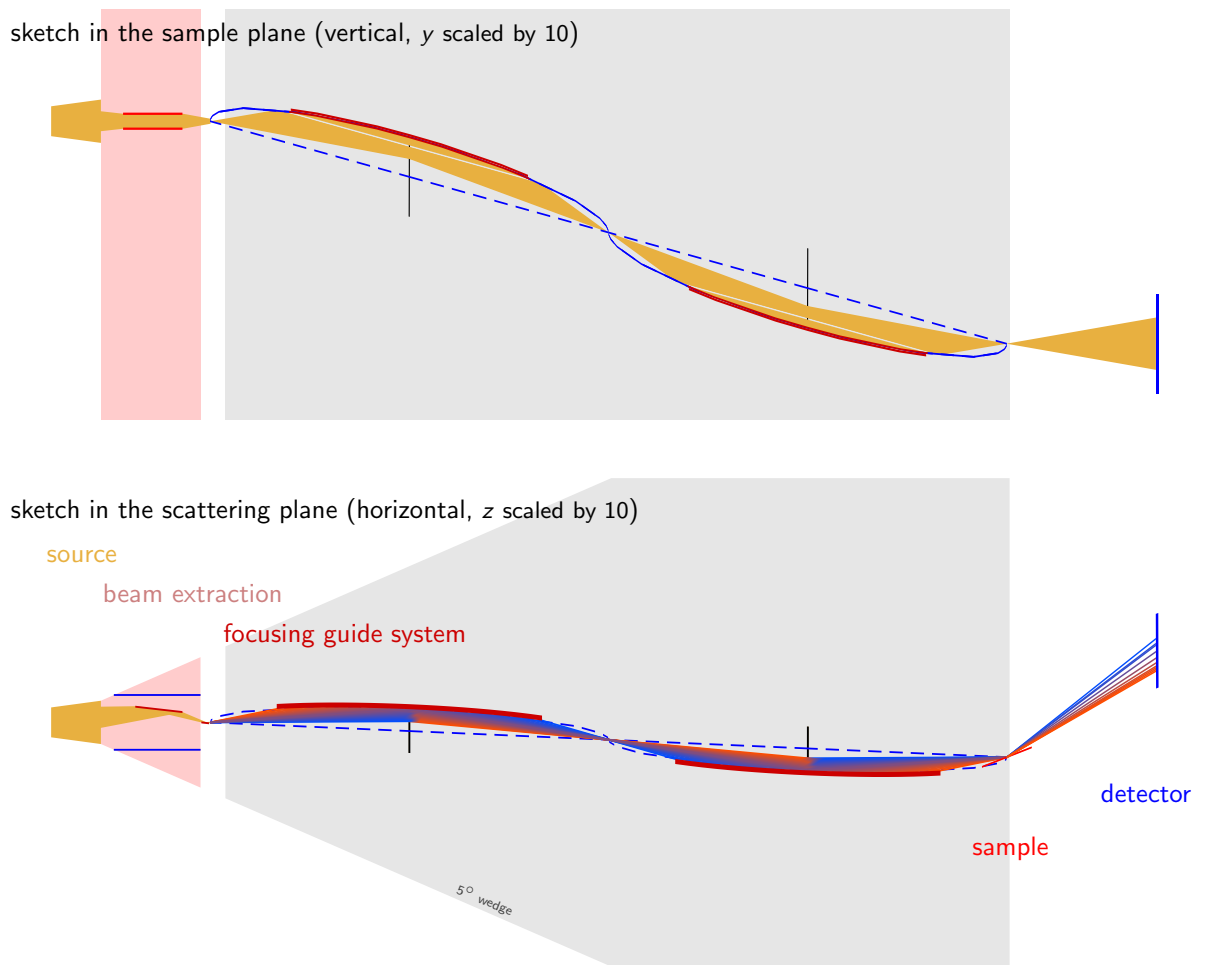


Figure 9: Schematic vertical and horizontal layout of the reflectometer with a horizontal scattering geometry, and with the first slit (P_1) outside the biological shielding. The gray wedge corresponds to a 5° segment, the light red areas are the biological and the instrument shielding. The parameters used for these sketches are $a_{xy} = a_{xz} = 8000$ mm, $b_{xy}/a_{xy} = 0.02$, $\Delta\theta_{xy} = 2^\circ$, $b_{xz}/a_{xz} = 0.011$, and $\Delta\theta_{xz} = 1.1^\circ$. The beam extraction lay out is the one discussed in section 2.2.2.

3.1 double-Selene guide system

This is an alternative approach to the one discussed above, paying respect to much higher shielding demands. If the biological shielding and the shielding around the first guide are not sufficient (as is claimed by the experts from ISIS and SNS), one can build a guide system with 2 subsequent *Selene* sections. The first looks on a fix pin hole in the extraction section and creates a small but homogeneous virtual source some 20 m to 30 m from the moderator. From there direct and first indirect line of sight is blocked efficiently. The beam is then manipulated (shaped, polarised, filtered) at or close to that virtual source point and fed into the second *Selene* guide system.

As a result, the guide dimensions are reduced by a factor 2, gravity effects are reduced by a factor 4, but the number of reflections in the guide increases from 4 to 8. This means that this approach favours longer wavelengths where the reflectivity of the coating is more efficient.

Following the argumentation of section 2.1 the usable wavelength range starts at about 5 \AA for this guide. With an instrument length of some 50 m this means that the wavelength range is $\lambda \in [5, 10] \text{ \AA}$. For the ESS baseline parameters this has the consequence that the background burst from the proton pulse appears at the beginning and the end of the used wavelength range. Further optimisation leads to the situation that the bursts are just outside the required λ range, as is sketched in figure 10.

For this scheme, the flight times for the shortest / longest wavelength are 73 ms / 137 ms (assuming a burst

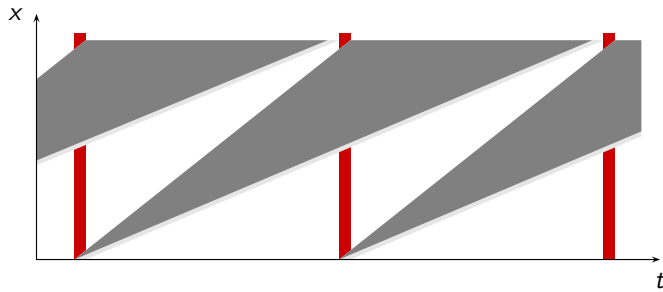


Figure 10: Sketch to illustrate how to avoid the influence of the γ and fast neutron burst from the proton pulse hitting the target. The sketch is to scale with period $T = 70$ ms, pulse length $t = 3$ ms, and a sample detector distance of 58 m, i.e. $\lambda \in [5, 9.3]$ Å.

time of 3 ms). For $\lambda_{\min} = 5.00$ Å this leads to an instrument length of $\overline{SD} = 58'400$ mm, and this in turn to $\lambda_{\max} = 9.38$ Å. The distance from moderator to the pin hole is $\overline{SP_1} = 4200$ mm (for $\Delta\theta = 1.5^\circ$, see section 2.2.3). Assuming a sample - detector distance of 6200 mm one ends with 48'000 mm for the 4 identical elliptic guides, i.e. each has to cover 12'000 mm. With $\xi = 0.60$ one gets the actual length of the guide elements of 7'200 mm. The guide parameters for these numbers are $b/a = 0.01754$, $c = 6'000$ mm, and the coating is of $m = 2.5$.

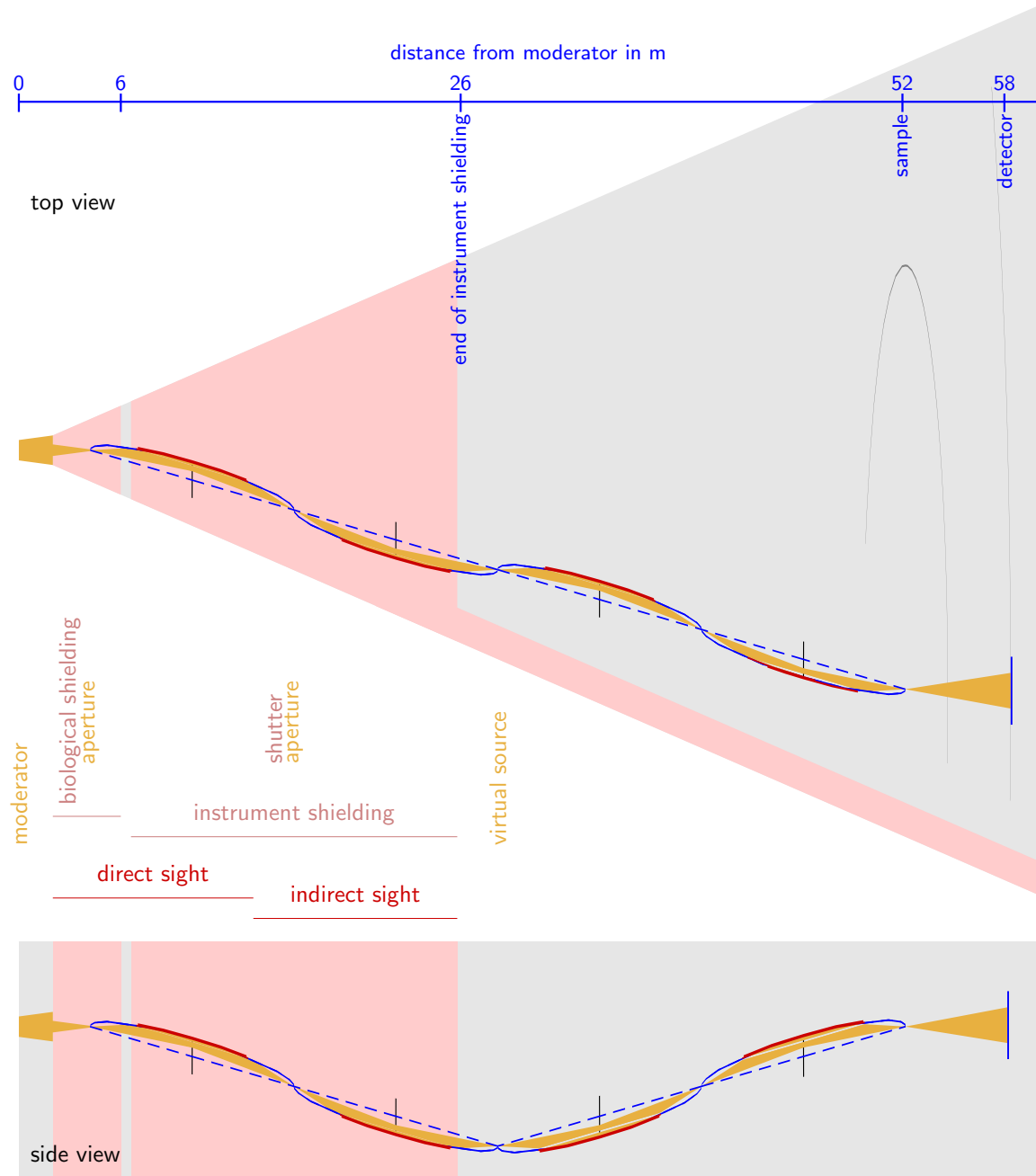


Figure 11: Sketch of a guide system with two subsequent pairs of ellipses. A small ($10 \times 10 \text{ mm}^2$) aperture 4.2 m from the source acts as the initial focal slit for the first *Selene* guides. These are completely within a shielding. Direct line of sight to the source is possible all along the first guide element. Secondary radiation can be directly seen all along the second guide element. Behind that the beam is focused down to the size of the initial aperture. At that point the precision shaping of the footprint is performed. The second *Selene* guide acts as in the set-up described above. This way the shielding ends some 26 m after the moderator. The beam channel is bent several times so that the radiation level should be much reduced. The polariser or a band-pass filter will be positioned in a low-radiation region easily accessible for maintenance.

5 prototype

This section is under construction. Most of the subsections are empty and wait for being filled.

5.1 BOA

instrument description
physical parameters

5.2 design considerations

length of the focusing section (4a): The available space is some 9 m. About 3 m are needed to get an acceptable angular resolution on the detector ($\Delta\theta \approx 0.04^\circ$). Another 1.5 m before the first focal point are required for the ml-monochromator, the chopper and eventually further equipment. This leads to $4c = 4$ m.

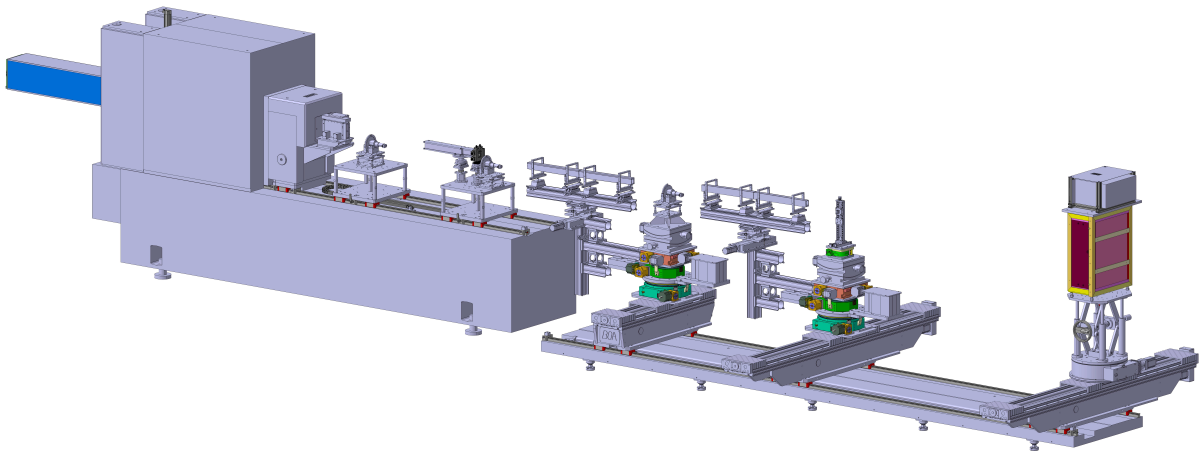


Figure 13: Assembly drawing of the construction of the *Selene* prototype set-up on the test facility BOA at PSI. The elements/devices from left to right: n-guide of BOA; pulse chopper on table 2; double ml monochromator, precision slit, pulse chopper (alternative position) on table 3; first guide section on support system, attached to table 4; frame overlap chopper on table 4; second guide section on support system, attached to table 5; sample holder on yz translation stage on table 5; and area detector on table 6.

5.3 devices

Most of the following devices were designed, constructed and fabricated at PSI. The Exceptions are the X95 elements, the precision slit and the guide elements.

5.3.1 pulse chopper

The reduced length of the set-up compared to the ESS dimensions with about the same λ range leads to shorter repetition rate and pulse length for the test set-up. The pulse chopper will be operated with up to 60 Hz, its open/closed time ratio is about 5% (to be determined exactly).

The much reduced dimension of the beam relative to conventional set-ups leads to a disc diameter of $\varnothing = 160$ mm. The absorbing material is 2.2 mm of an Al :¹⁰ B alloy, followed by 2 mm Cd. The absorbing region is 10 mm wide. Figure 14 shows on the left side the pulse chopper after assembling, before testing.

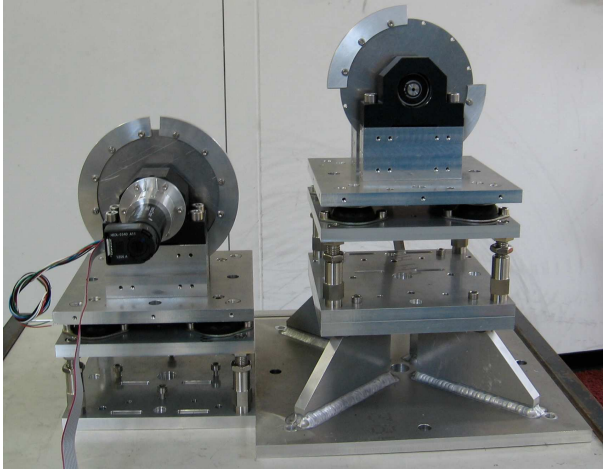


Figure 14: Pulse chopper (left) and frame overlap chopper (right) for the *Selene* prototype.

5.3.2 frame overlap chopper

The frame overlap chopper has similar dimensions as the pulse chopper, but a open/close time ratio of 50%. Its position will be at or close to the intermediate focal point of the *Selene* guide system. The frame overlap chopper is the left device in figure 14.

5.3.3 precision slit

The small dimensions of the prototype results in a down-scaling of the sample and thus of the slit at the first focal point. The beam cross section is of the order $0.1 \times 1 \text{ mm}^2$. This will be realised with a precision x-ray slit system, equipped with BorAl and Cd absorbers. The slit is custom made by ACS and based on their system !!!.

5.3.4 double multilayer monochromator

The double multilayer monochromator consists of 2 borcron glass substrates, coated with a Ni/Ti multilayer with a first order peak at $m = 3$ with $\Delta q/q = 7\%$. The surfaces are mounted parallel face to face with a gap of 6.5 mm. The first substrate is 305 mm long, the second 119 mm. In x direction there is a 5 mm gap in between both. The design is optimised for a slit positioned 43 mm behind the end of the device. The acceptance is $\Delta\theta = 1.8^\circ$ for $\lambda \in [4, 10] \text{ \AA}$.

The device was tested and characterised on Amor. Since the divergence available for this test was only of the order of 0.3° , the full angular range was reached by tilting the monochromator in discrete steps. Figure 15 shows the resulting $I(\theta, \lambda)$ map. The width of the intensity streak shown here is limited by the measurement range, not by the device.

To characterise $\Delta\lambda/\lambda$ and the off-specular scattering, also measurements were performed with a well collimated beam (slits of 1 mm opening, 100 mm and 2200 mm from the entrance of the device). The $I(\lambda)$ curves for various θ is shown in figure 16.

Figure 17 shows the off-specular scattering for $\lambda = 6.3 \text{ \AA}$ with various slit positions and openings behind the device. The slits before the ml-monochromator are 1 mm each. Surprisingly there is the same broad diffuse background with an exponential decay for all measurements. The origin is unclear yet, but eventually this is a feature of the detector.

5.3.5 sample holder

The sample holder is simply an Al cuboid with grooves and slits to insert (glue) the sample and some absorbing sheets. It is mounted on a y and z translation stage.

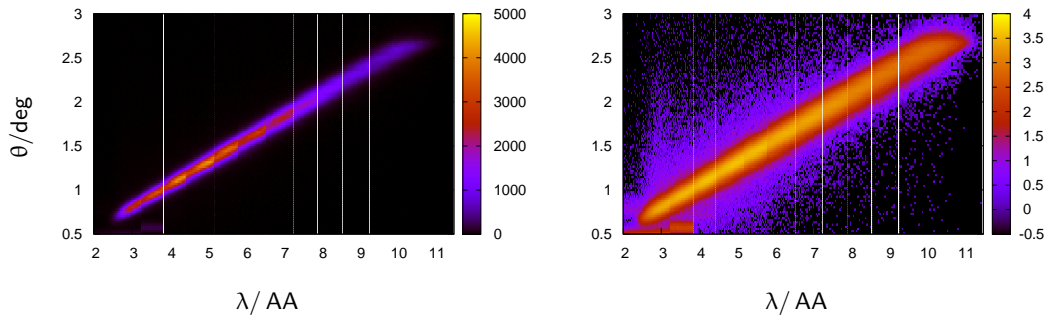


Figure 15: $I(\lambda, \theta)$ on linear (left) and logarithmic scale (right) obtained with the ml-monochromator on Amor. The maps are stitched together from 11 measurements since the incoming divergence was limited to 0.3° .

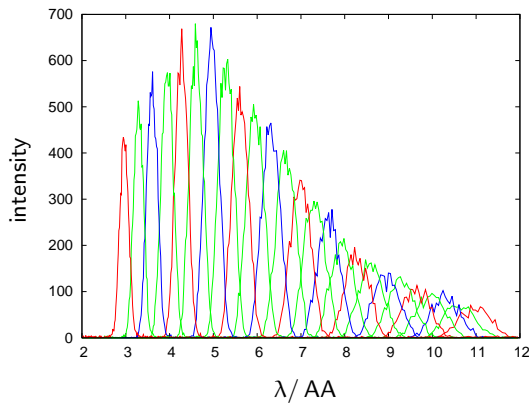


Figure 16: $I(\lambda)$ for $\theta = 0.5^\circ, 0.6^\circ, \dots, 3.0^\circ$. The varying height of the individual scans reflects the λ -dependence of the intensity of the incoming beam.

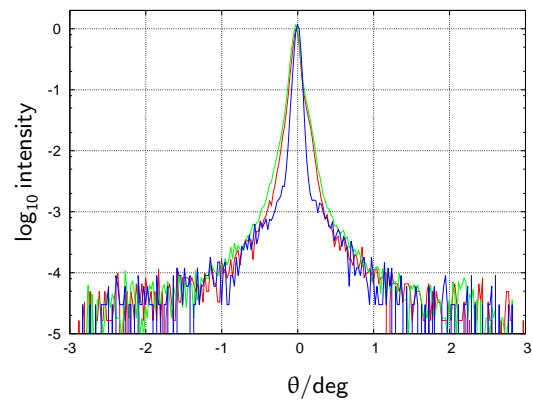


Figure 17: $\log_{10}[I(\theta)]$ without aperture behind the device (green), with a 0.5 mm aperture at 50 mm (red), and with a 1 mm aperture at 1300 mm (blue).

5.3.6 guide support

The guide support system is assembled from X95 profiles and joints, motorised and manual translation tables and manual tilting stages. Figure 18 shows the mounting frames for the single guide elements (figure ??), the height and tilt-adjustments and the X95 bar where upon the guide elements are mounted. This bar is positioned on tilting- and translation stages, which are to be mounted to the lower rotation stages of the BOA tables 3 and 4, respectively.

5.3.7 guide system

The *Selene* guide system in this case consists of 2 sections focusing elliptically in two dimensions (i.e. in y and in z), where each section consists of 2 mirror-inverted elements of 600 mm length. Figure 20 shows one guide element before mounting.

The device was constructed and build by SwissNeutronics according to the measures $c = 1000$ mm, $b/a = 0.0\dots$, $\xi = 0.60$, coating Ni/Ti with $m = 4$. The horizontally reflecting glass substrate has a constant height of 46 mm. The vertically reflecting glass has one straight edge along the optical axis, and one elliptically curved edge, fitting the horizontal reflectors shape. The vertical reflector has a minimum width of 21 mm.

5.4 set-up

not yet realised (will start on 13. August 2012)

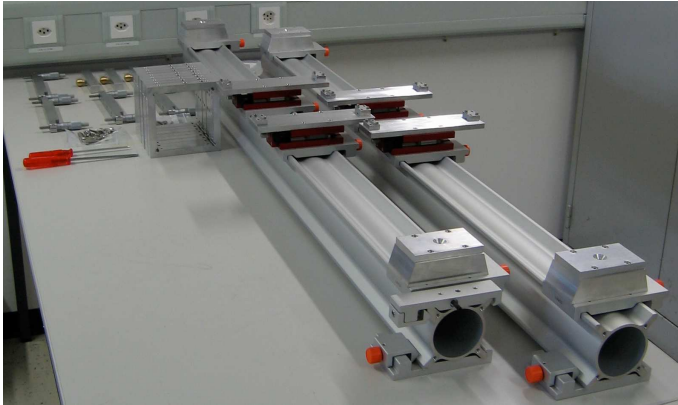


Figure 18: Parts of the guide support before mounting the guide elements.

Figure 19: Guide support with 2 guide elements mounted. Shown is the second guide of the *Selene* set-up, reflecting left and downwards. The guides are not yet adjusted, the knife blade slit is missing.



Figure 20: Single guide element (half a guide section). The blue part is an L-shaped Al bar on which the glass substrates are screwed. The Al frames are for mounting the elements on the support and alignment system.

5.5 experiments

not yet performed (will start on 20. August 2012)

6 publications

The *Selene* concept and experimental results were published as refereed manuscripts, as oral presentations and on posters. The following table chronologically lists publications and reports connected to this work.¹

reviewed publications

- 2012 *Focusing specular neutron reflectometry for small samples*
J. Stahn, U. Filges, T. Panzner
European Physical Journal - Applied Physics **58**, 11001 (2012)
DOI:10.1051/epjap/2012110295
- 2011 *Neutron reflectometry by refractive encoding*
R. Cubitt, J. Stahn
Eur. Phys. J. Plus **126**, 111 (2011)
DOI:10.1140/epjp/i2011-11111-0
- *Study on a focusing, low-background neutron delivery system*
J. Stahn, T. Panzner, U. Filges, C. Marcelot, P. Böni
Nuclear Instruments and Methods A **634**, S12 (2011)
DOI:10.1016/j.nima.2010.06.221
- 2009 *Focusing of cold neutrons*
— *performance of a laterally graded and parabolically bent multilayer*
M. Schneider, J. Stahn, P. Böni
N.I.M. A **610**, 530-533 (2009)
DOI:10.1016/j.nima.2009.08.047

oral presentations

- 2012/07 *Selene — a focusing guide system*
J. Stahn, et al.
Institut Laue-Langevin, workshop on Neutron Delivery Systems
9. - 11. July 2012 Grenoble, France
- 04 *progress report of the Swiss-Danish instrument initiative for the ESS*
J. Stahn
IKON 3, 18. - 19. 04. 2012, Berlin, Germany
- 04 *Selene*
J. Stahn
ESS workshop on elliptic neutron guides, 17. 4. 2012, Berlin, Germany
- 03 *concept for a reflectometer using focusing guides*
J. Stahn, T. Panzner, U. Filges
TUM & FRM II seminar, 12. 03. 2012, München, Germany
- 02 *progress report of the Swiss-Danish instrument initiative for the ESS*
WP2: focusing reflectometer
J. Stahn
IKON 2, 09. - 10. 02. 2012, Malmoe, Sweden
- 01 *Concept for a reflectometer for the ESS with focusing in the sample plane and in the scattering plane*
J. Stahn, U. Filges, T. Panzner
Workshop on off-specular neutron scattering, 09.-10. 01. 2012, Bruxelles, Belgium

¹The presentations are linked or deposited for download on the web-page
<http://people.web.psi.ch/stahn/publications.html>.

- 2011/10 *TOF reflectometry at PSI: from an optical bench set-up to a new instrument concept with a focus on small samples*
 J. Stahn
 JCNS instrumentation workshop, 04. -07. 10. 2011, Tutzing, Germany
- 09 *concept for a reflectometer for the ESS with focusing in the sample plane, and a convergent beam in the scattering plane*
 Jochen Stahn
 meeting of the ESS reflectometry TAP, 15. 09. 2011, Lund
- 09 *concept, design and first results: convergent-beam reflectometry using a focusing elliptic guide*
 Jochen Stahn, Uwe Filges, Tobias Panzner, Martie Cardenas, Beate Klösgen
 IKON-1, First In-Kind Contributions Meeting for Neutron Science for the ESS
 8. 9. 2011, Lund, Sweden
- 07 *Selene: high-intensity specular reflectometry*
 J. Stahn, U. Filges, T. Panzner
 5th European Conference on Neutron Scattering, ECNS 2011
 July 17.-22. 2011, Prague, Czech Republic
- 2010/06 *specular reflectometry on small samples using a convergent beam*
 J. Stahn
 reflectometer seminar, Oslo, 17. 06. 2010
- 05 *study on a focusing, low-background neutron delivery system*
 J. Stahn, T. Panzner, U. Filges
 JCNS seminar, Garching, 04. 05. 2010
- 03 *study on a focusing, low-background neutron delivery system*
 J. Stahn, T. Panzner, U. Filges
 neutron optics workshop NOP2010, Alpe d'Huez, 17.-19. 03. 2010
- 2008/06 *elliptic neutron guides - from the idea to the implementation*
 J. Stahn
 nmi3 meeting 2008, Corse, France: JRA3 - Neutron Optics
- 06 *laterally graded and complex multilayers for neutron optical elements*
 J. Stahn
 nmi3 meeting 2008, Corse, France: JRA3 - Neutron Optics
- 04 *elliptic beam guide - concept and first tests*
 J. Stahn
 ILL workshop on neutron guides, 26., 27. 04. 2006, ILL, Grenoble
- poster**
- 2012/04 *Science and Scientists @ ESS - conference: 19th-20th of April, 2012, Berlin, Germany:*
Selene-type reflectometer — principle
Selene-type reflectometer for small samples
Selene-type reflectometer — prototype on BOA
 J. Stahn, T. Panzner, U. Filges, M. Cardenas, B. Klösgen, U. Bengaard Hansen